Age-dependent prediction of visible differences in displayed images

Rafał K. Mantiuk
Giovanni Ramponi

***Abstract* —** A comprehensive computational model of the human visual system has been developed to predict just-noticeable differences between a pair of stimuli. The stimuli are provided as high-dynamic-range, multichannel images, containing accurate spectral and photometric description of the scene. In this work, we extend such a model to determine the effect of age on the sensitivity of the visual system. The extensions are based on the existing models of disability glare, aging of the crystalline lens, and reduced pupil size with age (senile miosis). We confirm findings from other studies that those optical effects cannot fully explain the effect of aging, and we attribute the remaining drop of sensitivity to neural changes. The complete model, including an empirical neural component, can well explain the differences in contrast sensitivity between old and young observers.

Keywords — *human vision model, aging effects, visual difference prediction.*

1 Introduction

Many practical applications require predicting contrast detection and discrimination thresholds in complex images. For example, it is often desirable to compress an image using lossy compression in such a way that the compression artifacts are unnoticeable to the observer. To achieve this goal, the original image and the image with compression distortions can be analyzed by a *visibility predictor* in order to determine whether the distortions are noticeable for an average observer and decide to adjust the compression rate accordingly. Visibility predictors are also used to compare and evaluate the results of algorithms that generate the pair of test and reference images, such as image and video compression methods and techniques for denoising and deconvolution. In computer graphics, visual predictors are used in adaptive rendering, where the computation is directed to those image regions for which the improvement in quality is the most noticeable. They can also be exploited to design energy-saving displays that maintain good perceived image quality.[1,2]

Visibility predictors[3–6] assess the likelihood that an average observer will notice the difference between the test and reference images. Test images usually contain, and reference images lack, features whose visibility is investigated. Such features could be compression distortions, artifacts of computer graphics algorithms, or text that is tested for legibility.

A problem with such predictors is that they do not match the visual performance of a particular individual. This is because the performance can differ substantially between people while the visibility predictors are trained with the data averaged over a group of observers.

Age is an attribute that is easy to specify and has strong influence on the visual performance of an individual. Although age alone does not fully explain individual variations, it can explain a significant portion of those. Therefore, in this paper we improve the performance of a visibility predictor, namely, HDR-VDP-2, by incorporating age-related changes in visual performance. We review the existing models determining the impact of age on visual performance, and we incorporate them in the predictor based on their fit to the data. The initial results of this work were presented in Mantiuk and Ramponi.[7]

2 Visual difference predictors

The performance of the human visual system (HVS) in detecting and discriminating luminance contrast patterns has been one of the most thoroughly researched areas in vision science. But, despite a substantial body of research and data, few of the proposed models can claim to predict visual system performance for arbitrary complex stimuli seen in any viewing conditions. The majority of the models are meant to explain the data for only very simplistic stimuli, such as sine gratings or Gabor patches, usually seen on a uniform background of constant luminance.

Daly[3] proposed one of the first comprehensive visual predictors intended to work with complex images—the visual difference predictor (VDP). The predictor includes a comprehensive model of the contrast sensitivity function (CSF), spatial-selective and orientation-selective cortical bands, visual masking, and pooling detection probabilities across bands. An alternative CSF was proposed by Barten,[8] who collated data from a number of contrast sensitivity studies

Accepted 01/10/18.
Rafał K. Mantiuk is with the Computer Laboratory, University of Cambridge, Cambridge, UK.
Giovanni Ramponi is with the DIA, University of Trieste, Via Valerio 10, Trieste, Italy; e-mail: ramponi@units.it.

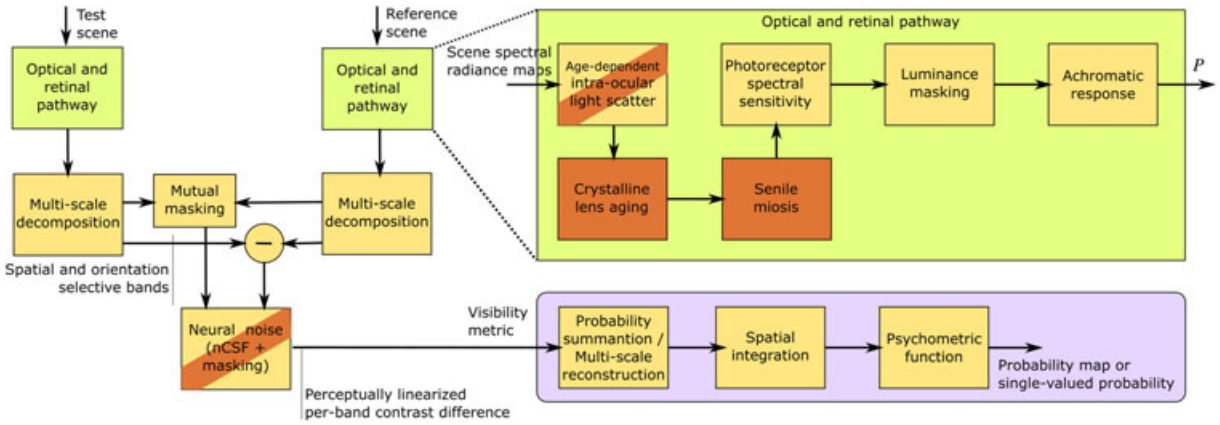

FIGURE 1 — The data flow diagram for the visual model (HDR-VDP-2). The new components that account for the aging effects are shown in orange (dark) and the components that have been extended to account for age are marked with an orange diagonal band. nCSF, neural contrast sensitivity function.

and derived a model of optical, retinal, and neural processing. The model found many uses; for example, it has been adopted for the DICOM gray-scale function[9] used in medical diagnostic displays. The visual discrimination model[4] is another influential visual predictor, which includes the effect of the eye's optics causing disability glare.[10] Instead of elevating the neural noise threshold as performed in VDP, visual discrimination model uses the concept of contrast transducers[11] to model contrast masking. Based on similar concepts, Pattanaik *et al.*[12] built the visual model for color `images. However, the focus of that work was tone mapping and color reproduction in varying viewing conditions rather than accurate measurement of visibility thresholds.

One of the obstacles in the development of robust visual models for complex images is the lack of data that could be used to validate them. Two examples of an effort to collect such data are the ModelFest initiative for luminance detection patterns[5] and the discrimination and masking data set for complex images.[13]

The majority of visual models are meant to predict performance only in a restricted range of physical luminance levels, often limited to either photopic or scotopic vision. This is partly because most modern psychophysical data come from studies conducted on cathode ray tube monitors, which operate in a limited range of luminance, usually from 0.1 to 80 cd/m^2. However, many applications require visual models that can account for a much broader range of luminance.[14] The VDP for high-dynamic-range images (HDR-VDP)[15] is one of the first visual models intended to operate on differences in scenes that contain large variation of absolute luminance levels. The HDR-VDP extends the original Daly's VDP by incorporating the disability glare, nonlinear response of the photoreceptors for the full visible range of luminance, and the CSF, which adapts to the spatially localized luminance patch rather than assuming a single adaptation level per image. Because the strength of the age-related loss of sensitivity depends on the absolute luminance level, HDR-VDP is a good candidate for testing age-dependent models. In fact, in this work we employ the second revision of HDR-VDP, which we describe in the next section.

2.1 HDR-VDP-2

HDR-VDP-2[6] is the second revision of the VDP for high-dynamic-range images, which offers better accuracy. We selected this model because (a) it operates in the required range of luminance; (b) it was shown to predict well a large range of experimental data; and (c) the investigated age-dependent effects can be easily incorporated into the publicly available source code.* In the following paragraph we give an overview of the model, while the details can be found in Mantiuk *et al.*[6]

The architecture and the data flow of the VDP are shown in Fig. 1. The predictor consists of two identical visual models: one for processing a test image and another for a reference image. For example, for visibility testing, it could be a windshield view with and without a pedestrian figure. For measuring detection, the pair consists of an image with and without a stimulus, both at the same background luminance level.

Because visual performance differs significantly across the luminance range as well as the spectral range, the input to the visual model needs to precisely describe the light entering the pupil. Both the test and reference images are represented as a set of spectral radiance maps, where each map has its associated spectral emission curve. In a simple case of viewing a computer monitor, it could be the spectral emission of the monitor and the linearized values of its primaries.

The first stage of the system—*optical and retinal pathway* (refer to Fig. 1)—simulates the optical properties of the eye and the receptor response. Most of the age-dependent components are introduced at that stage (shown in orange in the diagram). The light entering the eye is scattered, thus causing *disability glare*. Then, the retinal illumination is further reduced because of the age-related effects. The light reaching the retina is absorbed by the receptors (L-cones, S-cones,

*The source code can be found at http://hdrvdp.sf.net/.

M-cones, and rods) according to their spectral sensitivities. The varying sensitivity of the receptors to light is simulated as *luminance masking*, and the responses from rods and cones are combined into a single *achromatic response*.

There is ample evidence for the existence of mechanisms that are selective to narrow ranges of spatial frequencies and orientations. To mimic such a decomposition, which presumably happens in the retina and the visual cortex, the HDR-VDP-2 employs a *multi-scale image decomposition*, which is based on a steerable pyramid. The model assumes that the discrimination performance is limited by the neural noise, which consists of two components: a signal-independent neural contrast sensitivity function (nCSF) and the signal-dependent masking signal. The detected signal is the difference between the bands from test (B_T) and reference (B_R) images that is normalized by the overall amount of neural noise. Such difference is computed as follows:

$$D[f,o] = \frac{|B_T[f,o] - B_R[f,o]|^p}{\sqrt{N_{\mathrm{nCSF}}^{2p}[f,o] + N_{\mathrm{mask}}^2[f,o]}}, \quad (1)$$

where f and o are the indices of spatial and orientation bands and p is the parameter controlling the masking (usually $p = 3.5$). All uppercase symbols denote two-dimensional matrices with images. The neural contrast sensitivity component, N_{nCSF}, is the function of spatial frequency and the masking component, N_{mask}, is the function of both test and reference bands (mutual masking).[6] It is affected by the current visual band (self-masking) and by the neighboring bands (cross-channel masking).

Finally, the differences D from multiple bands are pooled together using probability summation and transformed into probabilities using a psychometric function.

3 Reference data

In order to evaluate different models of visual system aging, which we will review in the next section, it is necessary to collect a test data set. Such a data set will be used to validate the predictions of the reviewed models. We decided to reconstruct the measurements of the spatial contrast sensitivity of Sloane *et al.*,[16] which were obtained for two age groups: young observers with the average age 24 and elderly observers with the average age 73. The CSF measurements were selected as they capture the holistic performance of the visual system near the threshold and can be reliably measured. The data of Sloane *et al.*[16] are adequate for our purpose as it capture the drop of sensitivity with age as a function of both a spatial frequency and an absolute luminance level. These factors are the most relevant for testing sensitivity in complex images. Moreover, the measurements were made in relatively natural (although monocular) viewing conditions with a natural pupil and refraction corrected for the target distance. Such measurements better correspond to real-world visual performance than the data captured with an artificial pupil.

To prepare the test set, we created floating point images, stored in a high-dynamic-range OpenEXR format, which provides sufficient accuracy for low-contrast detection data. We assumed the spectral emission of a typical cathode ray tube display and matched the luminance levels with those reported in the paper. The original Sloane *et al.*[16] measurements and the HDR-VDP-2 predictions for the younger age group are shown in Fig. 2. The predictions are relatively good, given that no calibration was made to improve the fit. The largest difference between the data and the predictions can be found for 2–4 cpd and the highest luminance of 107 cd/m^2. We suspect that this is because Sloane *et al.*[16] used a temporarily modulated stimuli (0.5 Hz) while HDR-VDP-2 was calibrated with stationary Gabor patches (0 Hz).

4 Models of visual system aging

In this section, we review the models that account for the effect of aging on vision and report their influence on predictions when incorporated into the HDR-VDP-2. For a more complete treatment of the topic, please refer to the excellent reviews in Schieber[17] and Owsley.[18]

4.1 Disability glare

A small portion of the light that travels through the eye is scattered in the cornea, lens, inside the eye chamber, and on the fundus.[10] Such scattering causes a light pollution that reduces the contrast of the light projected on the retina. The effect is pronounced when observing scenes of high contrast containing sources of strong light. The effect is commonly known as disability glare[19] and has been

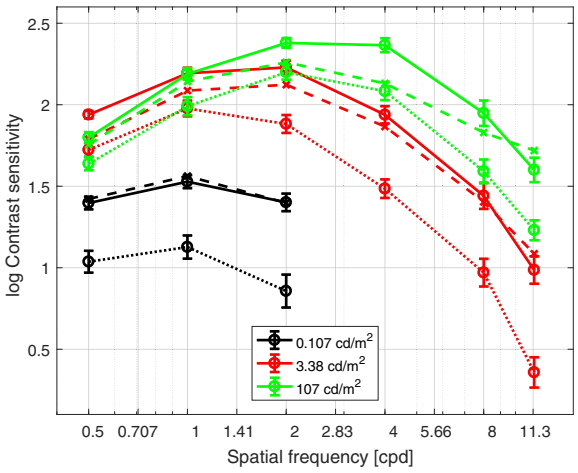

FIGURE 2 — The contrast sensitivity function as reported in Sloane *et al.*[16] for three luminance levels (different line colors), for 24-year-old (continuous line, circles) and 73-year-old (dotted line, circles) age groups. The dashed lines with the "x" markers show the HDR-VDP-2 prediction (no age-dependent extensions) for the 24-year-old mean observer.

thoroughly measured using both direct measurement methods, such as the double-pass technique,[20] and using psychophysical measurement, such as the equivalent veiling luminance method.[10] The measurements performed for different age groups clearly indicate that the effect of glare is stronger for elderly observers.[10]

The model of the disability glare that is particularly suitable to be incorporated in the proposed system is based on the measurements of Vos[10] and Vos and van den Berg.[19] The GSF is conceptually similar to a point spread function of the eye; however, the model is based on psychophysical rather than physical measurements. The actual point spread function of the eye's optics may differ substantially from the GSF.

To incorporate an age-dependent model of glare in the HDR-VDP-2, the original intraocular scatter function has been replaced with the age-dependent Commission Internationale de l'Eclairage (CIE) glare spread function (GSF)[19] (refer to Fig. 1). We used the most accurate formula from the recommendation [eq. (8) in Vos and van den Berg[19]], which is valid for the angles between 0.1° and 100°.

The visual glare is simulated as a convolution with a linear filter. However, constructing a digital filter based on GSF is not a trivial task as the function has a steep slope near 0° eccentricity. Therefore, it is necessary to sample that region very finely. To derive the digital filter values, we compute eight samples per minute of the visual arc and integrate the fraction of scattering using the trapezoidal method. Because the GSF is isotropic, the one-dimensional filter is expanded into two-dimensional after accounting for the increased integration area with eccentricity. As the GSF has a very wide support, it is convenient to perform filtering in the Fourier domain. To account for the cyclic property of the Fourier transform, we construct a modulation transfer function kernel of double the size of an image, and we pad the image with the average image luminance. A digital filter is then transformed into the Fourier domain and used to filter the input image.

The effect of age on the glare is shown in Fig. 3, which visualizes the difference in sensitivity between the young and elderly eye based on the CIE model incorporated in the HDR-VDP-2. The plot shows only a minor drop in sensitivities, up to 0.04 $\log_{10}$ units for 11.3 cpd pattern. The performance is nearly the same for all three luminance levels as glare is modeled as a linear filter, independent of the absolute light level. The small differences are mostly due to nonlinearities in the further stages of the system. The effect is slightly stronger for higher frequencies. It should be noted, however, that the employed glare model may be less accurate for high spatial frequencies, and it does not account for the changes in modulation due to the pupil size. Although the pupil size is included in some of the proposed modulation transfer functions of the eye (see, for example, Watson[21]), those models are based on the data collected for healthy young eyes and do not account for the changes due to aging.

Our goal is to make the predictions (continuous lines) match the data of Sloane *et al.*[16] (dashed lines in Fig. 3). From the plot, it is clear that the disability glare alone cannot account for the loss of sensitivity observed in the elder population. It must be noted, however, that the effect of glare may be much more significant for different stimuli, in particular for dark scenes that contain strong sources of light in eccentricity. Because light sources can be orders of magnitude brighter than diffuse objects in a scene, even a small amount of scattered light significantly reduces contrast in the dark parts of the scene. Therefore, we decided to include the age-dependent model of glare in the predictor despite its small effect for our test data.

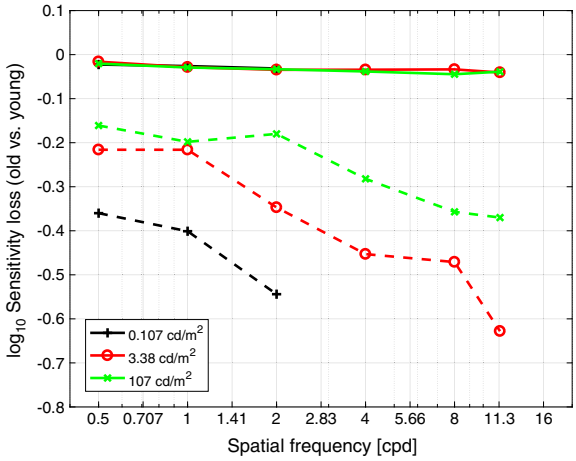

FIGURE 3 — The predicted loss of sensitivity due to disability glare (solid lines). The plotted values indicate the difference in sensitivity between elderly (mean 73 years) and young (mean 24 years) observers. Different line colors and markers denote different luminance levels. Note that disability glare has very small effect in sensitivity, which is almost identical for all luminance levels and almost independent of spatial frequency. The dashed lines show the measurements of Sloane *et al.*,[16] which indicate a much stronger drop in sensitivity for older observers and a significant variability of this drop with respect to both spatial frequency and luminance.

4.2 Aging of the crystalline lens

Lens aging effects are among the most significant contributions to changes in vision over time. Apart from suffering from a reduced accommodation ability, the lens increases its optical density with time. Such increase in density varies with respect to light wavelength. Both accommodation and density changes are because in the entire lifespan, the lens continues to generate new fibers; its older parts become compacted and accumulate in the central region of the lens itself, making it less transparent and more rigid. A chemical–physical analysis of the process is offered in Michael and Bron.[22] These physiological changes often turn into pathology, leading to cataracts of different types.

Pokorny *et al.*[23] proposed a model of lens aging in terms of optical density. The authors rely mainly on the data from a study in Stiles and Burch[24] for the age range 16–55 and a study in Moreland[25] that extends to age 13–83; they demonstrate that the change in density is different at different wavelengths (the spectral density of the elderly lens is not a scalar multiple of the earlier density) and that the rate of density

increase can be modeled by two different equations for age values below and above 60.

The relevant computations take as a reference an average 32-year-old subject. The subject's total density of the lens O_D, a dimensionless quantity corresponding to the logarithm of the transmission function, is deemed because of the sum of two contributions: O_{D1}, affected by aging after age 20, and O_{D2}, a constant residual. O_{D1} and O_{D2} values are provided as tables, derived from data by Stiles and Burch[24] and by several other studies.

Specifically, the total optical density O_D as a function of age is determined as

$$O_D(a) = \begin{cases} O_{D1}(1 + 0.02 \cdot (a - 32)) + O_{D2} & \text{if } a \leq 60 \\ O_{D1}(1.56 + 0.0667 \cdot (a - 60)) + O_{D2} & \text{if } a > 60 \end{cases}, \quad (2)$$

where a denotes age in years, and O_{D1} and O_{D1} are the values from Pokorny *et al.*,[23] which are reported in Table 1 for convenience. The resulting lens transmission function, expressed as $TF = 10^{-OD}$, is plotted in Fig. 4 on a semilog scale as a function of light wavelength, for 20 to 80 years of age.

We have introduced the model of aging of crystalline lens into the HDR-VDP-2, as a wavelength-dependent optical filter (refer to Fig. 1), which reduces the light that reaches the retina. The effect is straightforward to integrate with HDR-VDP-2, as the model already operates on spectral data and accounts for the spectral sensitivities of the photoreceptors. The model from Eq. (2) is used to find the corrected transformation from the input colors space of N-primaries (usually $N = 3$), into the response of cones (L, M, and S) and rods.

TABLE 1 — Data for optical density contributions, from Pokorny *et al.*[23]

Wavelength (nm)	O_{D1}	O_{D2}
400	0.600	1.000
410	0.510	0.583
420	0.433	0.300
430	0.377	0.116
440	0.327	0.033
450	0.295	0.005
460	0.267	0
470	0.233	0
480	0.207	0
490	0.187	0
500	0.167	0
510	0.147	0
520	0.133	0
530	0.120	0
540	0.107	0
550	0.093	0
560	0.080	0
570	0.067	0
580	0.053	0
590	0.040	0
600	0.033	0
610	0.027	0
620	0.020	0
630	0.013	0
640	0.007	0
650	0	0

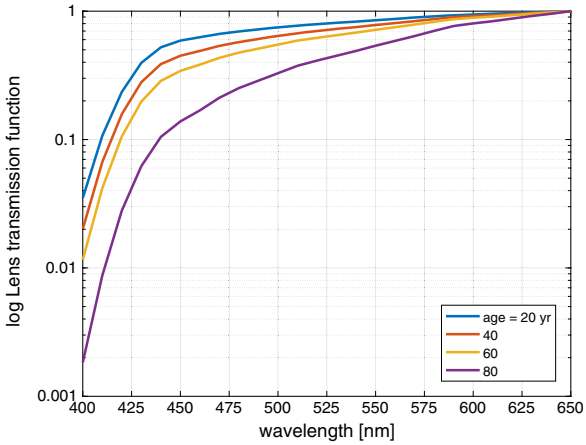

FIGURE 4 — Lens transmission function at different ages, based on the model from Pokorny *et al.*[23]

The solid lines in Fig. 5 show the sensitivity loss as predicted by the modified HDR-VDP-2. It can be seen that the effect is strong at lower luminance levels (0.107 cd/m^2) and is almost negligible at the photopic levels. This is because the worsened lens transmission at older age results mostly in reduced retinal illumination. Photopic vision is little affected by the overall changes in the retinal illumination (as the consequence of the Weber law); however, in the mesopic and scotopic vision range below 3 cd/m^2, the sensitivity gradually decreases with decreasing retinal illuminance. It is worth noting that it is possible to make such observation only after the model of aging of crystalline lens is integrated with the complete visual predictor. The model alone does not explain the luminance dependency of its effect. When compared with Sloane's measurements (dashed lines in Fig. 5), it is obvious that the reduced lens transmission alone cannot explain the overall loss of sensitivity at older age.

4.3 Senile miosis

The diameter of the pupil controls the illuminance of the retina and is therefore an important component in HVS models.

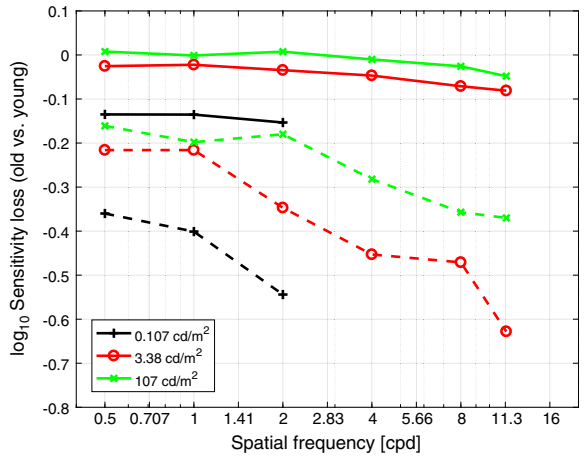

FIGURE 5 — The predicted loss of sensitivity due to aging of crystalline lens (solid lines). Other lines and markers are the same as in Fig. 3.

Several models exist that represent the relationship between the pupil diameter and the luminance of an extended light source placed in front of the observer, when other light sources are absent or have negligible effect.[8,26,27] These models have been derived from the experiments performed mainly between the 1920s and the 1950s and in some cases assemble the results obtained by different authors. They yield pupil diameter versus luminance plots that have an aspect similar to the one in Fig. 6. More sophisticated models take into account the field size (in deg^2) of the source and differentiate between monocular and binocular viewing. A comprehensive review of these studies is presented in Watson and Yellott.[27]

As the eye becomes older, the average diameter of the pupil for a given value of illumination tends to become smaller. The effect is known as senile pupillary miosis. In dim light, the diameter at age 80 can be one-half of the one at age 20; it has also been estimated that, at age 60, retinal illuminance is reduced by 0.3 log units with respect to young subjects.[17] An obvious cause of this phenomenon would be the reduced elasticity of the iris, but recently, it was suggested that miosis could rather be an attempt of the HVS to increase retinal contrast and overall visual performance, counteracting the effects of increased intraocular light scattering[17] and of the consequent glare. If we were to model improved retinal contrast because of smaller pupil size,[21] we would expect to see increased sensitivity for older population, especially at lower luminance levels. The data of Sloane *et al.*[16] indicate the opposite that the sensitivity for high frequencies is reduced with age. So the reduced pupil diameter merely compensates for degradation of optical quality of the eye with age.

Probably the most ample experiment that relates age and pupil diameter is the one reported in Winn *et al.*[28] Ninety-one healthy subjects in the age range 17–83 underwent pupil diameter measurements performed using an infrared-based continuous recording technique. Subjects were exposed to five different luminance sources at 9, 44, 220, 1100, and 4400 cd/m^2. Some 450 data points were obtained that, notwithstanding a significant dispersion, show a clear trend: For a given luminance, the diameter becomes smaller with increasing age; the effect is visible at all luminance levels but is stronger at low levels. A slope value was determined by the authors, in mm/year of age, for the linear fit to the relation between pupil diameter and age, at each of the five adapting luminances.

Based on the data of Winn *et al.*[28] and using Stanley and Davies'[29] model of a pupil size, Watson and Yellott[27] derived a comprehensive unified formula. The formula predicts the diameter of the pupil, $S(\cdot)$ (mm), as the function of adapting luminance [L (cd/m^2)], age [a (years)], and field area [f (deg^2)]:

$$S(L,a,f) = (a - 28.58)\,(0.02132 - 0.009562\,D_{\mathrm{sd}}), \quad (3)$$

$$D_{\mathrm{sd}} = 7.75 - \frac{5.75\,k}{k+2}, \quad (4)$$

$$k = \left(\frac{Lf}{846}\right)^{0.41}. \quad (5)$$

The function is plotted for two age groups in Fig. 6. The plot indicates 2.5-mm reduction in the diameter and 65% reduction in retinal illuminance between 24- and 73-year age groups for low luminance.

Senile miosis can be readily incorporated in the HDR-VDP-2 as a factor that limits retinal illumination. Because HDR-VDP-2 was calibrated for a young eye and a natural pupil, the factor is computed as the ratio $S(L,a,f)/S(L,24,f)$, where $S()$ is the function from Eq. (3).

Figure 7 shows the HDR-VDP-2 predictions with the incorporated model of senile miosis. The sensitivity change is almost independent of the spatial frequency. The two lower luminance levels show a significant drop of sensitivity, while the highest luminance of 107 cd/m^2 is not affected. Similar as for the other effects, the effect of senile miosis alone cannot explain the data of Sloane *et al.*[16]

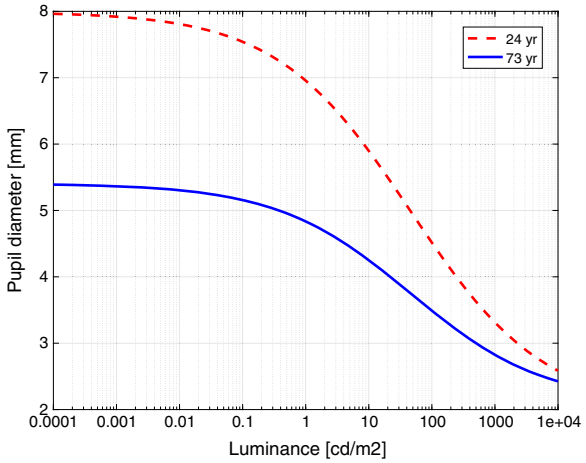

FIGURE 6 — Pupil diameter versus adaptation luminance for two age groups, according to the two tested models.

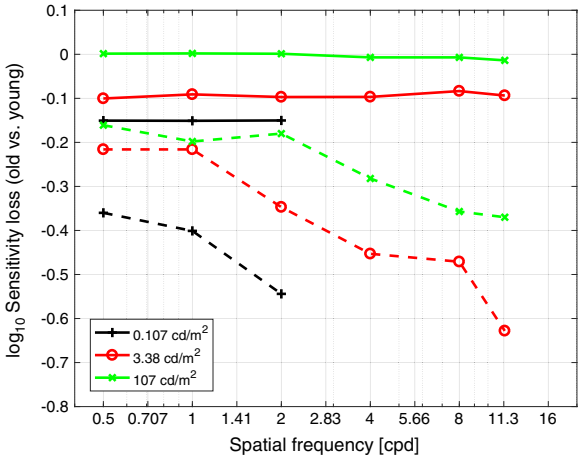

FIGURE 7 — The predicted loss of sensitivity due to senile miosis (solid lines). Other lines and markers are the same as in Fig. 3.

4.4 Combined optical model

As shown in the previous section, none of the age-dependent factors could fully explain the sensitivity drop between young and old age groups in Sloane *et al*.[16] data. Now, we investigate whether the combined influence of these factors can explain the data. It is important to notice that all the effects are mostly independent. Reduced pupil diameter is not affected and does not affect aging of crystalline lens. The pupil size will affect glare. However, the CIE GSF was measured for natural pupils, so the function already incorporates the effect of pupil size.

Figure 8 shows the combined effect of age-dependent glare, aging of crystalline lens, and senile miosis. The plot shows that even when all these factors are combined, the predictions (continuous lines) still do not match the data (dashed lines). This is visible for the high luminance level of 107 cd/m^2 and for low spatial frequencies, where all factors predict almost no loss of sensitivity, while the data indicate 0.16 log-10 unit drop.

4.5 Neural changes

Looking at Fig. 8, it could be rather surprising that none of the discussed factors affect significantly sensitivity at 107 cd/m^2. However, this result is easy to explain. All the considered factors reduce the amount of retinal illumination. Because the luminance of 107 cd/m^2 is in the Weber region of the luminance sensitivity curve, the sensitivity stays constant despite the significant loss of retinal illumination. Therefore, such a loss of sensitivity can be only explained by changes affecting receptors and neural mechanisms. A similar conclusion was also made by Sloane *et al*.[16] and Elliott *et al*.,[30] who found that "an explanation based solely on light absorption differences in the young vs. old eye is inadequate in explaining older adults contrast sensitivity deficit." In general, studies agree that age-related decrease in CSF cannot be ascribed to optical reasons only (miosis and lens opacification) and must have a neural-related cause. The age-related decrease in rod cell density and in ganglion cell density are logical candidate causes, although no psychophysical data have supported this explanation.[18]

Burton *et al*.[31] directly measured the loss of sensitivity between young and old observers using laser interferometry, a technique that bypasses the optics of the eye in presenting a gratings target on the retina. They found a moderate loss of sensitivity, between 0.1 and 0.2 log. Such a loss could explain the difference between the predictions and the data in Fig. 8.

Instead of modeling Burton *et al*.[31] data, which the authors admit are noisy, we fit an empirical model that alters the neural CSF component of the HDR-VDP-2 (refer to Fig. 1). A good fit can be achieved for the linear function of the logarithmic spatial frequency:

$$\log_{10}(\Delta S) = -\big(\beta \log_2(\rho + \alpha)\big) \cdot \max(a - 24, 0), \qquad (6)$$

which describes the changes in log-10 sensitivity for the age (a) in years and spatial frequency (ρ) in cpd. The value ΔS is added to N_{nCSF} from Eq. (1) to alter the amount of neural noise. The best fit was achieved for the parameters α = 0.75 and β = 0.00195. The result of that fitting can be found in Fig. 9. Although it could be possible to achieve a better fit with a more complex function, that would result in overfitting to the data that is affected by noise and other factors.

The empirical neural component much improves the fit to the data. Still, the model underpredicts the sensitivity loss for low spatial frequencies and the highest luminance (107 cd/m^2). This could be due to a number of factors, including differences in stimuli (0.5 Hz temporal modulation versus static grating) or a higher loss of sensitivity of the rod-mediated mechanism. Owsley[18] notices that although most aging effects can be ascribed to optical rather than neurological causes, in scotopic and mesopic vision, neurological causes become more important. This observations are confirmed by Clark *et al*.[32] However, we did not attempt to further extend the

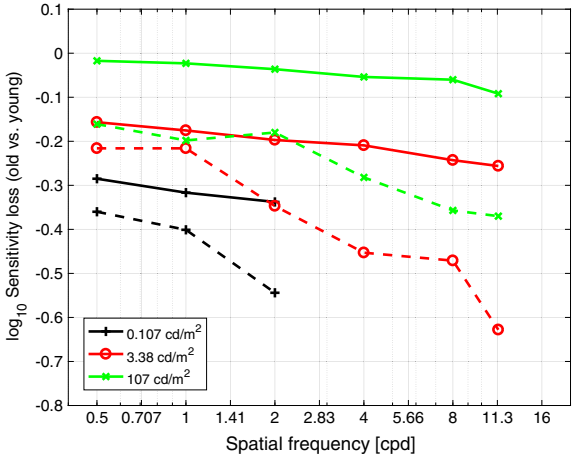

FIGURE 8 — The predicted loss of sensitivity due to combined effect of age-dependent glare, aging of crystalline lens, and senile miosis (solid lines). Other lines and markers are the same as in Fig. 3.

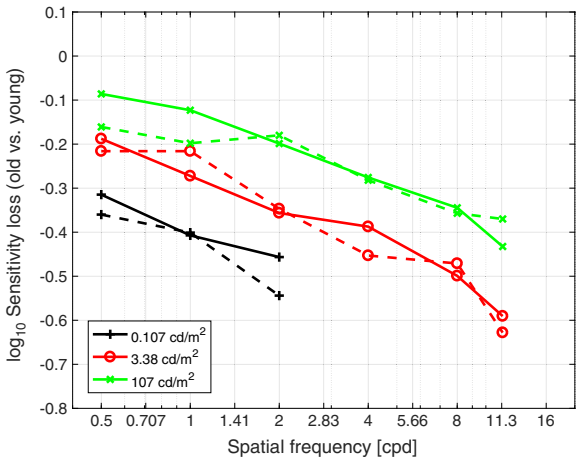

FIGURE 9 — The predicted loss of sensitivity due to all factors included in Fig. 8 with the addition of the empirical sensitivity loss from Eq. (6) (solid lines). Other lines and markers are the same as in Fig. 3.

model from Eq. (6) as the available data are not sufficient to justify a more complex model.

4.6 Contrast masking and supra-threshold vision

Because we tested our model only with near-threshold sine-gratings, it is important to determine whether its predictions extend to supra-threshold contrast, which can be found in complex scenes. The measurement of contrast discrimination thresholds for young and elderly observers[33,34] has shown that age differences in supra-threshold contrast discrimination can be explained by age differences in contrast sensitivity. This means that when contrast is normalized by the age-dependent sensitivity (CSF), there is no measurable difference between both age groups. Because such normalization is a part of the HDR-VDP-2 contrast masking model, we can assume that its output is correct also for supra-threshold stimuli.

5 Discussion

The presented study makes three contributions towards better understanding the effect of age on vision. Firstly, it reviews and evaluates the performance of the existing partial models that consider aging of the visual system. The models are cross-validated against the data from another study, which was not used to derive these models. Secondly, we demonstrate that a complete model of detection and discrimination (HDR-VDP-2) is a useful tool for studying partial models of isolated effects, such as the model of disability glare, aging of crystalline lens, and senile miosis. Visual models are often proposed as stand-alone components, intended to predict one set of data. By incorporating these models in a more comprehensive visual model, we can test how the predicted effects interact with other components of the visual system.

Finally, we provide a practical visibility predictor that can estimate an average loss of sensitivity with age and thus improve predictions for individual observers. The predictor can be used in all applications that require adjusting system parameters for an age group. For example, medical displays should ensure that the just-noticeable differences in the visualized values are equally visible for young and older readers. In that case, the predictor could be used to derive an optimum gray-scale display function[9] for a particular age of a reader. Another application is the prediction of age-dependent visual performance in vision-critical applications, such as driving. Figure 10 shows a scene from a driving simulator, in which we introduced three barely noticeable cats. Our model predicted that while all three cats will be visible to a younger driver, one of the cats will not be visible to a hypothetical elderly driver. We also incorporated the same visual model into an image luminance retargeting technique, intended for visualization of night scenes on much brighter displays.[35] Figure 11 visualizes the same night-driving scene as seen by 20- and 80-year-old observers. These pictures also hint that our model could be used even in image analysis applications, to tailor the analysis process to the needs and abilities of elderly users.

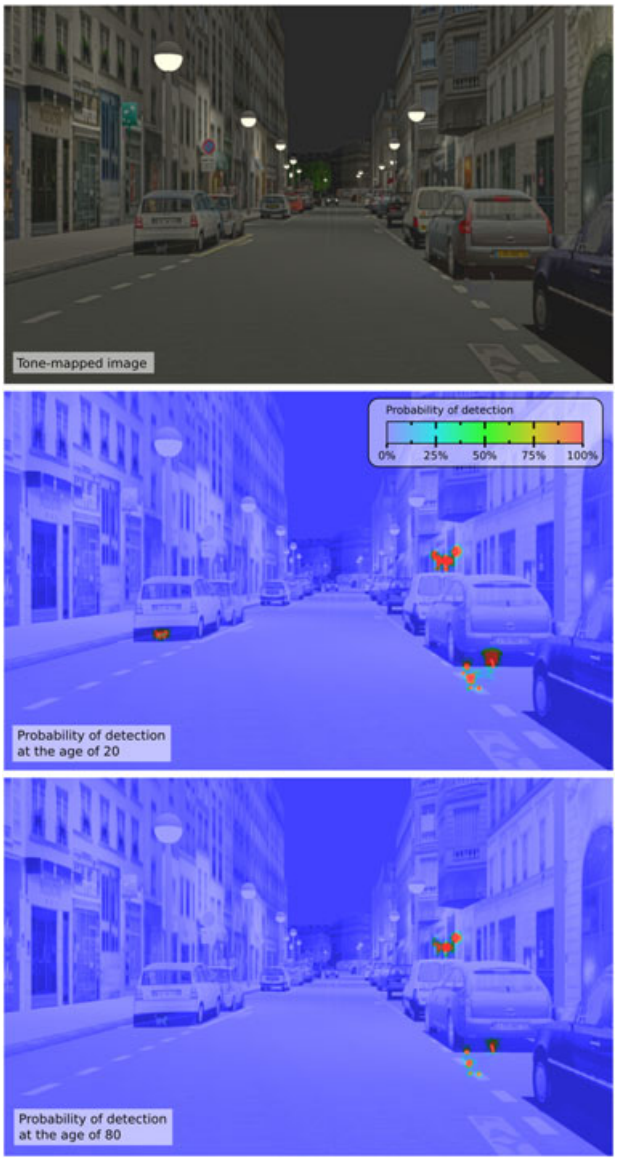

FIGURE 10 — The differences in visibility depending on age in a night-driving scenario. Three cats were added to an HDR image, which was rendered by a driving simulator. The two false-color maps show the HDR-VDP-2 predictions for the difference between the image with and without cats. The maps show that the cat on the left under the car is visible to a hypothetical 20-year-old driver but is not visible to a hypothetical 80-year-old driver. Note that the tone-mapped image on the top does not convey visibility in an actual scene and is included only for illustration purposes only.

5.1 Limitations

It is important to notice several limitations of this study. Firstly, all conclusions are based on fitting to a single set of measurements of Sloane *et al.*[16] Such measurements are limited to gray-scale stimuli that are near the detection threshold. The stimuli do not contain high contrast images that could test the influence of disability glare on vision in older observers.

FIGURE 11 — Visualization of night vision for 20- and 80-year-old observers. Note the increased amount of glare and reduced sensitivity for the 80-year-old observer.

The stimuli also do not contain chromatic components that could test the effect of increased density in a short wavelength in older observers. More data need to be collected for different age groups in order to obtain a more comprehensive and reliable data set for validation of visual models.

Secondly, all studies involving older observers struggle to differentiate between the vision changes that are the natural result of aging and those that are due to pathologies. Despite the efforts, some vision-related diseases may be undetected when screening participants for the experiments. But even if such strict screening could be implemented, it is disputable whether carefully screened observers constitute a representative sample for a given age group. Owsley[18] discusses this issue as the blurry border between physiology and pathology, referring to it as "a continuum of aging and disease."

Finally, it is necessary to point out large variations in sensitivity between individual observers, even within a single age group. Most studies on the effect of age report strong overlap between young and old age groups.[31,36] This means that a portion of older observers actually demonstrate a better visual performance than some younger observers. Therefore, it is important to recognize that the model captures the overall trend for an average observer, which may not reflect the performance of a random individual.

6 Conclusions

In this work we extended the visibility predictor, which is a comprehensive model of HVS sensitivity, to include the effect of aging. The extensions are mostly based on the existing age-dependent models, which consider distinct components of the visual system: pupil diameter, lens opacity, and disability glare. We confirm the observation made in other studies that the reduction in sensitivity cannot be explained by optical effects alone. The drop of sensitivity must also have neural bases, which influence the vision stronger at the scotopic and mesopic light levels.

The model and the data predict reduced sensitivity with age, with stronger reduction for higher frequencies and for lower luminance levels. It is, however, important to note that the effect of age on the average observer is moderate and can be smaller than the differences in sensitivity between individuals within the same age group.

The proposed model is capable of predicting detection and discrimination in arbitrary stimuli, including complex natural images. Such predictions rely on the assumption that the data measured for near-threshold detection tasks capture the overall changes in the HVS with age, including those that affect supra-threshold contrast detection. Further work needs to be performed to verify whether there are other age-related factors that affect the perception of complex natural scenes.

Future study will be devoted to tailor HVS-based models that expand the dynamic range of an image, such as Hong *et al.*,[37] in order to permit an easier adaptation to the requirements of different users.

Acknowledgments

G. R. appreciatively acknowledges many fruitful discussions and interactions with Dr. Gabriele Guarnieri. This work was supported by an internal research fund of the University of Trieste and by the EU Artemis Joint Undertaking project 100228 CHIRON.

References

1 C. Yang *et al.*, "A perceptually optimized mapping technique for display images," *J. Soc. Inform. Display*, **24**, No. 9, 576–586 (2016) [Online]. Available: https://doi.org/10.1002/jsid.501.
2 J. S. Park *et al.*, "Human visual perception-based localized backlight scaling method for high dynamic range LCDs," *J. Soc. Inform. Display*, **24**, No. 8, 471–486 (2016) [Online]. Available: https://doi.org/10.1002/jsid.458.
3 S. Daly, "The visible differences predictor: an algorithm for the assessment of image fidelity," in Digital images and human vision, A. B. Watson, (ed.). MIT Press, Cambridge, MA, USA, (1993), pp. 179–206.
4 J. Lubin, "A visual discrimination model for imaging system design and evaluation," in Vision models for target detection and recognition, A. Menendez and E. Peli, (eds.). World Scientific, Singapore, (1995), pp. 245–283.
5 A. Watson, "Visual detection of spatial contrast patterns: evaluation of five simple models," *Opt. Express*, **6**, No. 1, 12 (2000).
6 R. K. Mantiuk *et al.*, "HDR-VDP-2: a calibrated visual metric for visibility and quality predictions in all luminance conditions," *ACM Trans. Graph.*, **30**, No. 4, 1 (2011).
7 R. K. Mantiuk and G. Ramponi. Human vision model including age dependencies. in Proc. of EUSIPCO, 2015, pp. 1641–1645.
8 P. G. J. Barten, Contrast sensitivity of the human eye and its effects on image quality. SPIE Press, (1999).

9 DICOM, "DICOM part 14: grayscale standard display function. Medical Imaging and Technology Alliance, Tech. Rep.," (2011).
10 J. J. Vos, "On the cause of disability glare and its dependence on glare angle, age and ocular pigmentation," *Clin. Exp. Optom.*, **86**, No. 6, 363–370 (Nov. 2003).
11 H. R. Wilson, "A transducer function for threshold and suprathreshold human vision," *Biol. Cybern.*, **38**, No. 3, 171–178 (1980).
12 S. N. Pattanaik *et al.*, A multiscale model of adaptation and spatial vision for realistic image display. in Proc. of SIGGRAPH, 1998, pp. 287–298.
13 M. M. Alam *et al.*, A database of local masking thresholds in natural images. in *Human Vision and Electronic Imaging*, Mar. 2013, pp. 86510G-86510G-15.
14 M. A. Abebe *et al.*, "Perceptual lightness modeling for high-dynamic-range imaging," *ACM Trans. Appl. Percept.*, **15**, No. 1, 1:1–1:19 (2017) [Online]. Available: https://doi.org/10.1145/3086577.
15 R. Mantiuk *et al.*, Predicting visible differences in high dynamic range images: model and its calibration. in Human Vision and Electronic Imaging, 2005, pp. 204–214.
16 M. J. Sloane *et al.*, "Aging, senile miosis and spatial contrast sensitivity at low luminance," *Vision Res.*, **28**, No. 11, 1235–1246 (1988).
17 F. Schieber, "Vision and aging," in Handbook of the psychology of aging, M. G. James *et al.*, (eds.), 6th edn. Elsevier Academic Press, Burlington, MA, USA, (2011), pp. 129–154.
18 C. Owsley, "Aging and vision," *Vision Res.*, **51**, No. 13, 1610–1622 (Jul. 2011).
19 J. J. Vos and T. J. van den Berg, "CIE 135/1-6 disability glare," *Tech. Rep.*, **5**, 4 (1999).
20 P. Artal and R. Navarro, "Simultaneous measurement of two-point-spread functions at different locations across the human fovea," *Appl. Optics*, **31**, No. 19, 3646–3656 (1992).
21 A. B. Watson, "A formula for the mean human optical modulation transfer function as a function of pupil size," *J. Vis.*, **13**, No. 6, 1–11 (2013).
22 R. Michael and A. J. Bron, "The ageing lens and cataract: a model of normal and pathological ageing," *Phil. Trans. R. Soc. B*, **366**, No. 8, 1278–1292 (2011).
23 J. Pokorny *et al.*, "Aging of the human lens," *Appl. Optics*, **26**, No. 8, 1437–1440 (Apr. 1987).
24 W. Stiles and J. Burch, "N.P.L. colour-matching investigation: final report (1958)," *Opt. Acta*, **6**, No. 1, 1–26 (1959).
25 J. Moreland, "Temporal variations in anomaloscope equations," *Mod. Prob. Ophthalmol.*, **19**, 167 (1978).
26 S. de Groot and J. Gebhard, "Pupil size as determined by adapting luminance," *JOSA A*, **42**, No. 7, 492–495 (1952).
27 A. Watson and J. Yellott, "A unified formula for light-adapted pupil size," *J. Vis.*, **12**, No. 10, 1–16 (2012).
28 B. Winn *et al.*, "Factors affecting light-adapted pupil size in normal human subjects," *Invest. Ophthalmol. Vis. Sci.*, **35**, 1132–1137 (1994).
29 P. A. Stanley and A. K. Davies, "The effect of field of view size on steady-state pupil diameter," *Ophthalmic Physiol. Optics*, **15**, No. 6, 601–603 (Nov. 1995).
30 D. Elliott *et al.*, "Neural contribution to spatiotemporal contrast sensitivity decline in healthy ageing eyes," *Vision Res.*, **30**, No. 4, 541–547 (Jan. 1990).
31 K. B. Burton *et al.*, "Aging and neural spatial contrast sensitivity: photopic vision," *Vision Res.*, **33**, No. 7, 939–946 (May 1993).
32 C. L. Clark *et al.*, "Scotopic spatiotemporal sensitivity differences between young and old adults," *Ophthalmic Physiol. Opt.*, **30**, No. 4, 339–350 (Jul. 2010).
33 B. Beard *et al.*, "Contrast detection and discrimination in young and older adults," *Optom. Vis. Sci.*, **71**, No. 12, 783–791 (1994).
34 C. M. Fiacconi *et al.*, "The effects of aging on contrast discrimination," *J. Vis.*, **9**, No. 8, 1073–1073 (Mar. 2010).
35 R. Wanat and R. K. Mantiuk, "Simulating and compensating changes in appearance between day and night vision," *Trans. Graphics*, **33**, No. 4, 147 (2014).
36 J. IJspeert *et al.*, "The intraocular straylight function in 129 healthy volunteers; dependence on angle, age and pigmentation," *Vision Res.*, **30**, No. 5, 699–707 (Jan. 1990).
37 J.-J. Hong *et al.*, "Rendering of HDR images to improve brightness discrimination," *J. Soc. Inform. Display*, **24**, No. 1, 44–56 (2016) [Online]. Available: https://doi.org/10.1002/jsid.407.

Rafał K. Mantiuk received his PhD degree in computer science (summa cum laude) at the Max-Planck-Institut for Computer Science, Germany, in 2006, and his MSc degree in computer science at the Technical University of Szczecin, Poland, in 2003. He is a senior lecturer at the University of Cambridge, Computer Laboratory, UK, from 2015; a lecturer/senior lecturer at the Bangor University, School of Computer Science, UK, in 2009–2015; a postdoc fellow at the University of British Columbia, Canada, in 2008–2009; and a postdoc of the Max-Planck-Institut for Computer Science, Germany, in 2007–2008. He had his internship at the Sharp Laboratories of America, Camas, WA, USA, in 2006. His research interests include applied visual perception, high-dynamic-range imaging, display algorithms, tone mapping, video coding for new display technologies, image and video quality metric, visibility metrics, virtual reality and low-level perception, computational photography, computational displays, novel display technologies, color, perception in computer graphics, novel image and video representations (beyond 2D), psychophysics, and modeling visual perception with machine learning.

Giovanni Ramponi was born in Trieste, Italy, in 1956. He received his degree in electronic engineering (summa cum laude) in 1981. Since 2000, he has been the professor of electronics at the Department of Engineering and Architecture of the University of Trieste, Italy. His research interests include digital processing of images and image sequences, enhancement and feature extraction in images, image visualization, and image quality evaluation. Professor Ramponi was an associate editor of the IEEE Signal Processing Letters and of the IEEE Transactions on Image Processing. Presently, he is an AE of the SPIE Journal of Electronic Imaging. He has participated in various European and national research projects. He is the coinventor of several pending international patents and has published some 200 papers in international journals and conference proceedings, and as book chapters. Professor Ramponi contributes to graduate courses on digital signal processing. More details on www.units.it/ramponi.